Dynamically stable gallium surface coverages during plasma-assisted molecular-beam epitaxy of (0001) GaN

C. Adelmann, J. Brault, D. Jalabert, P. Gentile, H. Mariette, Guido Mula, B. Daudin

Growth Phase Diagram of (0001) GaN in Plasma-Assisted Molecular-Beam Epitaxy

C. Adelmann,[1] J. Brault,[1,2] D. Jalabert,[1] P. Gentile,[1] H. Mariette,[1,3] Guido Mula,[1,4] and B. Daudin[1,†]

[1] *Département de Recherche Fondamentale sur la Matière Condensée, SPMM, CEA/Grenoble, 17 Rue des Martyrs, 38054 Grenoble Cedex 9, France*

[2] *Laboratoire de Spectrométrie Physique, CNRS UMR C5588, Université Joseph Fourier – Grenoble I Boîte Postale 87, 38042 St.Martin d'Hères Cedex, France*

[3] *Laboratoire de Spectrométrie Physique, CNRS UMR C5588, Université Joseph Fourier Grenoble – Grenoble I Boîte Postale 87, 38042 St.Martin d'Hères Cedex, France*

[4] *INFM and Dipartimento di Fisica, Università di Cagliari, Cittadella Universitaria, Strada Provinciale Monserrato–Sestu km 0.700, 09042 Monserrato (CA), Italy*

The Ga surface coverage during the growth of GaN by plasma-assisted molecular-beam epitaxy is studied by reflection high-energy electron diffraction as a function of the Ga flux and the substrate temperature. As a consequence, a Ga surface coverage phase diagram is depicted. In particular, we show that a region exists in the diagram where the Ga surface coverage is independent of fluctuations in the Ga flux or the substrate coverage and which forms a "growth window" for GaN growth. The influence of the Ga surface coverage on the GaN surface morphology is discussed.

I. INTRODUCTION

The intense work on epitaxy of group III nitride materials for device applications is still contrasted by comparatively few studies on the physics of the growth itself. However, it is clear that thorough comprehension of growth mechanisms is a key issue for further improvement of the material quality. This is particularly true for plasma-assisted molecular-beam epitaxy (PAMBE) that still lags behind metal-organic chemical vapor deposition (MOCVD) as far as optical device growth is concerned. Especially, to date, no "growth window" has been established for GaN PAMBE, i.e. a region in growth parameter space that leads to optimized growth conditions independent of small parameter fluctuations.

The surface morphology of GaN layers grown by PAMBE has been found to depend strongly on the metal/N ratio: whereas films grown under metal-rich conditions generally exhibit smooth surfaces, as indicated by streaky reflection high-energy electron diffraction (RHEED) patterns, films grown under N-rich conditions show spotty RHEED patterns and rough surfaces [1–3]. In addition to surface morphology, material properties are also profoundly affected by the Ga/N ratio, N-rich growth being generally detrimental to both optical and electronic properties [1–3].

This effect has been explained in terms of adatom diffusion: it has been calculated that the diffusion barrier for Ga adatoms on N-rich surfaces is as high as 1.8 eV, whereas it is only 0.4 eV when the growth is carried out on a Ga-saturated surface [4].Thus, N-rich growth leads to very low adatom mobility and to an undesired kinetically-induced roughening of the surface. Recently, it has also been shown that the N adatom diffusion is significantly improved in Ga-rich conditions for surfaces covered by a Ga bilayer due to subsurface diffusion [5].

Thus, GaN growth by PAMBE is commonly carried out under metal-rich conditions. However, it has been found that, especially at low substrate temperatures, excess Ga sticks on the surface and forms droplets which block GaN growth underneath. This has been shown to be detrimental to material properties and a major drawback for device applications [2, 3, 6]. At higher substrate temperatures, an intermediate Ga-rich regime is observed, leading to smooth droplet-free surfaces [2, 3].

Recently, some works have elucidated the surface structure of the Ga-rich pseudo-1×1 surface generally encountered in Ga-rich GaN PAMBE. It has been shown by scanning tunneling microscopy (STM) [7] and RHEED [8] that this surface consists of an adsorbed Ga bilayer, in agreement with theoretical calculations [7, 9].

In the present article, we describe a growth phase diagram for homoepitaxial GaN grown by PAMBE. For this purpose, we assess the equilibrium Ga surface coverage on the GaN growth front as a function of substrate temperature and Ga flux. Furthermore, we discuss the surface morphologies and growth mechanisms that are observed for different Ga fluxes.

II. EXPERIMENTAL PROCEDURE

The experiments were performed in a commercial MECA2000 molecular-beam epitaxy growth chamber

[†] Corresponding author, electronic mail:bdaudin@cea.fr

equipped with a standard effusion cell for Ga evaporation. The active nitrogen was provided by an EPI Unibulb rf plasma cell. The pseudo-substrates used were 2 μm thick (0001) (Ga-polarity) GaN layers grown by MOCVD on sapphire. The substrate temperature T_S was measured by a thermocouple in mechanical contact to the backside of the molybdenum sample holder. Prior to all experiments, a 100 nm GaN layer was grown under Ga-rich conditions on the pseudosubstrates to prevent from the influence of a possible surface contamination layer. For all experiments described in the present article, the N_2 flux has been fixed to 0.50 sccm and the rf power to 300 W, which leads to maximum GaN growth rates of about 0.3 monolayers (ml) per second.

Ga fluxes have been calibrated by RHEED intensity oscillations during GaN growth at a substrate temperature of $T_S = 620$ °C in the N-rich regime. For these growth conditions, it has been found that the growth rate is actually proportional to the impinging Ga flux [10]. It is reasonable to suppose that the Ga adatom sticking coefficient is unity at such low substrate temperature which allows for an absolute calibration of the Ga flux.

The Ga surface coverage during growth was studied by analyzing the specularly-reflected RHEED intensity. We have previously shown that a Ga film desorbing from a GaN surface leads to an oscillatory transient that can be related to the Ga surface coverage [8]. The Ga surface coverage can then be qualitatively determined by stopping GaN growth and recording the variation of the specular RHEED intensity under vacuum. Although it is not always straightforward to assess an absolute Ga surface coverage, it is nevertheless possible to classify different regions in the surface coverage diagram.

GaN surface morphologies were determined by atomic-force microscopy (AFM) and STM after rapid sample cooling and transfer into air. Prior to STM imaging, the samples have been outgassed at 450 °C for about 1 h in an ultrahigh vacuum environment.

III. Ga SURFACE COVERAGE DURING GaN GROWTH

As it is common in III-V molecular-beam epitaxy, the GaN growth conditions will be described in terms of cation (Ga) flux and substrate temperature with a fixed active N flux. It is clear that a key parameter for GaN growth will be the Ga surface coverage ρ. To assess the Ga quantity present during GaN growth for different impinging Ga fluxes, the growth has been stopped after a definite time interval and the variation of the specular RHEED intensity has been subsequently measured during the excess Ga evaporation under vacuum.

Figure 1 shows the results after 90 s of GaN growth at $T_S = 740$ °C for different Ga fluxes Φ_{Ga}. At low Ga fluxes ($\Phi_{\mathrm{Ga}} < 0.3$ ml/s), the growth conditions are N-rich and only very few Ga atoms should be present on the growing surface. As a consequence, no variation of the specular RHEED intensity is observed after the growth.

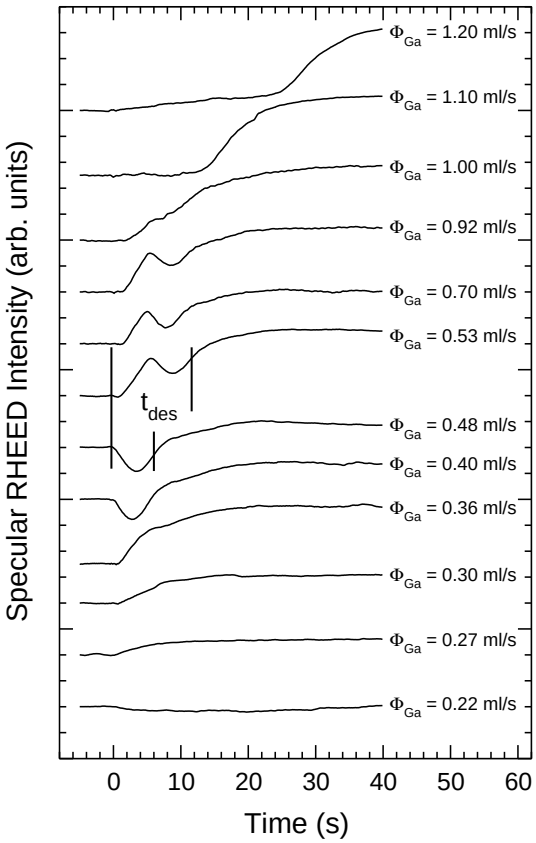

FIG. 1: Variation of the specular RHEED intensity during vacuum desorption of excess Ga after GaN growth at different Ga fluxes ($T_S = 740$ °C). The Ga desorption time t_{des} is defined as the delay between the GaN growth interruption and the inflection point of the last increase in RHEED intensity (full lines for $\Phi_{\mathrm{Ga}} = 0.48$ and 0.53 ml/s).

For higher fluxes, we observe oscillatory transients similar to those observed for Ga adsorption and desorption on GaN [8]. The transients are generally not independent of the Ga flux, but one can distinguish regions where they do not vary with the impinging Ga flux, e.g. between $\Phi_{\mathrm{Ga}} = 0.53$ ml/s and $\Phi_{\mathrm{Ga}} = 0.92$ ml/s.

At this point, it is important to note that for Ga fluxes below $\Phi_{\mathrm{Ga}} = 1.00$ ml/s the observed transients are also *independent of the previous growth time*. Even though the data presented in Fig. 1 have all been obtained after 90 s of GaN growth, identical transients have been observed after GaN growth at the same Ga fluxes during 30 s up to more than 1 h. Thus, the data in Fig. 1 are representative of (dynamically) stable Ga surface coverages of the GaN growth front and depend only on the Ga flux (i.e., the Ga/N ratio) and not on the specific choice of the growth time.

For Ga fluxes above $\Phi_{\mathrm{Ga}} = 1.00$ ml/s, we observe in

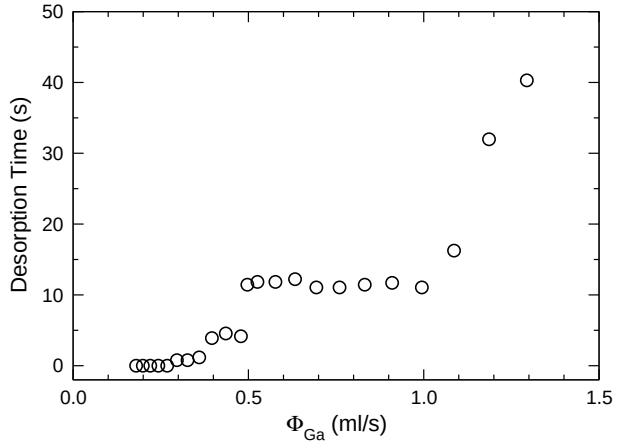

FIG. 2: Ga desorption time (dependent on the Ga surface coverage) after the growth of GaN for different Ga fluxes (T_S = 740 °C). Error bars are typically of the order of ±1 s.

Fig. 1 no initial change of the specular RHEED intensity, followed by an increase. However, the delay of the intensity increase is found to be dependent not only on the Ga flux (see Fig. 1) but also on the previous growth time, being longer for longer growth times. This indicates that excess Ga is continually accumulated on the growing GaN surface and will eventually form large Ga droplets by a ripening process [11].

As a consequence, the duration of the oscillatory transients in Fig. 1 can be used to classify the different dynamically stable Ga surface coverages. For this purpose, we have plotted the delay between the GaN growth interruption and the inflection point of the last increase in intensity for all curves where a variation of the specular RHEED intensity during Ga evaporation is observed. This desorption time is qualitatively related to the Ga surface coverage. The resulting data as a function of the Ga flux Φ_{Ga} are depicted in Fig. 2.

Below Ga fluxes of Φ_{Ga} = 0.3 ml/s, the growth conditions are N-rich, no variation of the RHEED intensity is observed after growth interruption, and the desorption time is zero. At higher fluxes, the growth conditions become Ga-rich, excess Ga is present at the surface and desorbs during the growth interruption. A first saturation of the Ga surface coverage is observed above Φ_{Ga} = 0.4 ml/s. When the Ga flux exceeds Φ_{Ga} = 0.5 ml/s, the desorption time, i.e. the Ga surface coverage during GaN growth, increases abruptly. It is worth noting that this transition between two different Ga surface coverages in dynamical equilibrium is non-continuous within our experimental resolution of 1 °C for the Ga effusion cell temperature, i.e. no stable intermediate Ga surface coverage has been found in our experiments.

Above Φ_{Ga} = 0.5 ml/s, the Ga surface coverage remains constant for a large range of Ga fluxes up to Φ_{Ga} = 1.0 ml/s. An identical oscillatory transient has been also found after Ga adsorption on GaN [8]. In the latter case, the amount of adsorbed Ga on the GaN surface was determined to be around 2.7 ml [8] (in terms of GaN surface site density) forming presumably a (laterally contracted) Ga bilayer on the GaN surface [9]. We can therefore conclude that Ga fluxes between Φ_{Ga} = 0.5 ml/s and Φ_{Ga} = 1.0 ml/s lead at T_S = 740 °C to a stable Ga bilayer coverage of the growing GaN surface.

At still higher Ga fluxes (Φ_{Ga} > 1.0 ml/s), no stable Ga surface coverage is observed. Excess Ga accumulates continuously on the growing GaN surface and finally forms liquid Ga droplets.

In summary, we can discriminate four different growth regimes:

A. N-rich growth with presumably negligible Ga surface coverage for $\Phi_{Ga} < 0.3$ ml/s,

B. Ga-rich growth with a Ga surface coverage of less than a Ga bilayer for $0.3 < \Phi_{Ga} < 0.5$ ml/s,

C. Ga-rich growth with a Ga bilayer adsorbed on the GaN surface (coverage of about ρ = 2.7 ml) for $0.5 < \Phi_{Ga} < 1.0$ ml/s, and

D. Ga droplet formation on top of the Ga bilayer for $\Phi_{Ga} > 1.0$ ml/s.

In the next section, we will present the variation of the Ga surface coverage with the substrate temperature, i.e. the GaN growth diagram. Finally, we will discuss the influence of the GaN growth conditions on growth mode, surface structures and material quality.

IV. GROWTH DIAGRAM

The experiments discussed in the previous section were obtained for GaN grown at a fixed substrate temperature

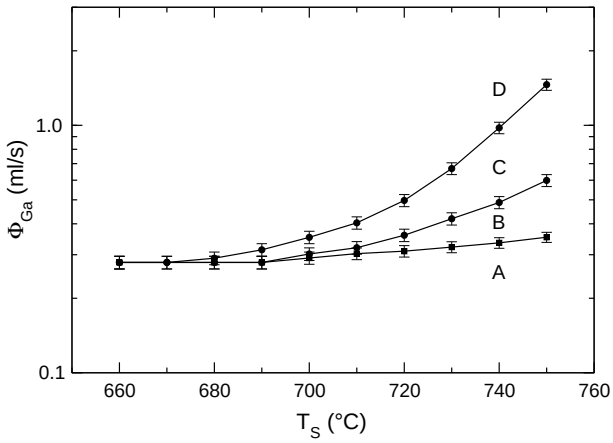

FIG. 3: GaN growth diagram indicating the Ga surface coverage during growth as a function of substrate temperature and Ga flux for fixed active N flux (0.3 ml/s).

of T_S = 740 °C. To obtain the GaN growth diagram, we have performed the measurements described above at various substrate temperatures in the range between T_S = 660 °C and T_S = 750 °C. The variation of the different growth regimes with substrate temperature is shown in Fig. 3. In general, higher substrate temperatures shift the different Ga rich growth regimes towards higher Ga fluxes.

In addition, we have determined the "Ga/N stoichiometry" by measuring the growth rate using RHEED oscillations for different Ga fluxes and substrate temperatures. For N-rich growth, the growth rate is limited by the impinging Ga-flux, increases with increasing Ga flux, and finally saturates at a Ga flux that will be defined as the "stoichiometric Ga flux" (see, e.g., Ref. 10). This flux coincides, within experimental precision, with the transition from N-rich to Ga-rich growth as determined by the Ga evaporation study described in the previous section. It has been found that the stoichiometric Ga flux increases only very slightly with the substrate temperature in the range considered in this study. This suggests that Ga reevaporation is weak under N-rich conditions, presumably owing to rapid incorporation due to a large number of available N atoms to form GaN.

In the most simple picture, the temperature dependence of the transition lines between the different Ga-rich growth regimes reflects the thermally-activated increase of Ga reevaporation from the GaN surface. All transition lines between N-rich growth (regime A), sub-bilayer Ga coverage (regime B), bilayer Ga coverage (regime C), and Ga droplet formation (regime D) can be fitted well with offset Arrhenius equations $\Phi = \Phi_i + A \cdot \exp(-E_A/kT_S)$ where the offset Φ_i takes into account the Ga incorporation into the growing GaN layer. Best fits lead to E_A = 2.4 eV, E_A = 3.7 eV and E_A = 4.8 eV for the transition lines between regions A and B, B and C, and C and D, respectively.

The activation energy of the transition line between N-rich and Ga-rich growth (regimes A and B) is close to that previously reported for Ga desorption from GaN (E_A = 2.2 eV, Ref. 12). This suggests that the increase of the stoichiometric Ga flux is due to thermally activated Ga reevaporation.

However, the activation energies corresponding to the transitions from regimes B to C and C to D, respectively, are much larger than the energies reported for Ga desorption from GaN (E_A = 2.2 eV, Ref. 12) or liquid Ga evaporation (E_A = 2.9 eV, see, e.g., Ref. 2). Furthermore, the value of E_A = 4.8 eV for the transition between the Ga bilayer regime C and the droplet regime D is much larger than a previously published value of E_A = 2.8 eV (Ref. 2). This suggests that the underlying physics of the GaN growth diagram is more complex than the proposed dynamic equilibrium between Ga adsorption and desorption [2] and kinetically-controlled processes, such as Ga droplet nucleation, may be crucial for a quantitative explanation. To address the difference between our measured activation energy for the transition between

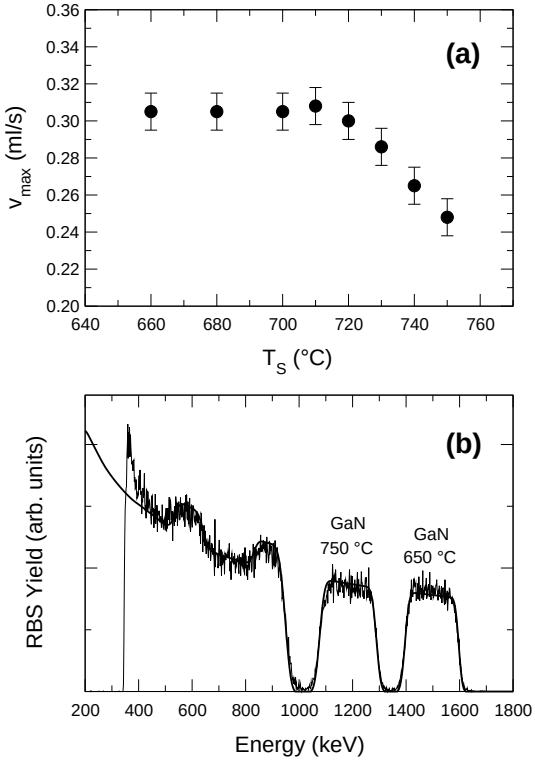

FIG. 4: **(a)** Maximum GaN growth rate $v_{\max}$ at the transition line between regions A and B as a function of substrate temperature. The maximum growth rate decreases above 710 °C due to GaN reevaporation. **(b)** RBS spectrum of a sample containing 2 layers of GaN grown for identical times at 650 °C in region D and at 750 °C in region C, respectively, and sandwitched between AlN layers.

regimes C and D and the previously reported result, it is worth noting that the N fluxes used in the present study are about four times lower than those in Ref. 2. We speculate that Ga droplet nucleation may not be completely independent of the impinging N flux. However, we stress that the Ga excess needed for droplet formation is of the same order of magnitude in both the present study and in Ref. 2.

Before we discuss GaN surface morphologies, we address the GaN growth rates in the different Ga surface coverage regimes. As already stated, the growth rate in the N-rich regime is proportional to the impinging Ga flux and saturates when the Ga/N stoichiometry is reached. Figure 4(a) shows this maximum growth rate as a function of the substrate temperature T_S. It is constant at lower temperature and decreases above about T_S = 710 °C. This behavior can be attributed to thermally activated GaN reevaporation. The growth rate loss at T_S = 750 °C is about 0.06 ml/s which is in good quantitative agreement with the GaN evaporation rate under vacuum of 0.08 ml/s in Ref. 13.

When the growth is carried out in the Ga bilayer or

droplet regime, no RHEED oscillations are observed (see below) and the growth rate must be determined by *ex situ* measurements of the layer thickness. This has been performed by means of Rutherford backscattering spectroscopy (RBS) using 2 MeV α-particles from a Van de Graaff ion accelerator. The backscattering angle was 165°. Figure 4(b) shows a RBS spectrum of two GaN layers grown for identical times at $T_S = 750$ °C in regime C and $T_S = 650$ °C in regime D, respectively, and sandwiched between AlN spacer layers. The thick solid line represents the result of a numerical simulation of the RBS spectrum. The thickness of the two layers is found to be identical within the experimental precision of about 1%, with a deduced growth rate of about 0.29 ml/s. We can therefore conclude that the growth rate in the Ga bilayer regime C is independent of the substrate temperature in the range explored in this article, contrary to the growth rate in the sub-bilayer regime B. It seems that the presence of the Ga bilayer prevents the decomposition of the GaN surface, similar to what has been observed for ammonia [13, 14]. This is corroborated by the observation that GaN surfaces quickly roughen when heated to 750 °C under vacuum due to GaN decomposition, while such roughening is not observed when the GaN surface is exposed to a Ga flux.

V. GaN SURFACE MORPHOLOGY

To study the surface morphologies corresponding to the different growth conditions, four 1 μm thick GaN layers have been grown by MBE on GaN templates at $T_S = 730$ °C in regions A,B,C, and D, respectively (see. Fig. 3). These samples have been characterized by AFM (samples A and B) and STM (samples C and D).

Figure 5(a) shows the AFM image of the surface of the sample grown in N-rich conditions (region A). During growth, Bragg spots gradually appeared in the RHEED pattern after about 300 nm of GaN growth. The surface morphology is characterized by inverted pyramids, about 50–80 nm deep, with $\{10\bar{1}3\}$ facets as sidewalls. Such facets are also weakly visible on the RHEED pattern of such a surface.

Figure 5(b) shows the AFM image of the surface of the sample grown under Ga-rich conditions with a Ga coverage of less than a bilayer (regime B). Like sample A, this sample also showed gradual Bragg spot appearance in the RHEED pattern after about 300 nm of GaN deposition. Interestingly, the surface is characterized by the same inverted pyramids formed by $\{10\bar{1}3\}$ facets, about a factor of 2 larger than those of the previous sample. This shows that the presence of few Ga excess atoms does not alter the driving force for pinhole formation.

The origin of these inverted pyramids formed during GaN growth in regimes A and B is still unclear. They appear similar to the "V-shaped" defects observed for GaN [15] and InGaN [16] growth, which are defined by $\{10\bar{1}1\}$

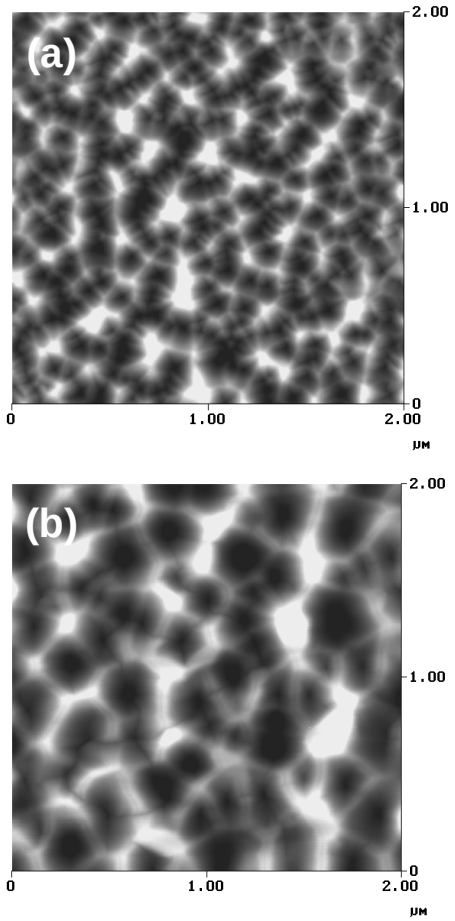

FIG. 5: Atomic-force micrographs of GaN surfaces grown under (a) N-rich conditions (growth phase diagram region A) and (b) slightly Ga-rich conditions (Ga coverage below a bilayer, growth phase diagram region B). The z-scales are 100 nm and 150 nm, respectively.

facets, though. Concerning these V-shaped GaN defects, it has been proposed that differences in the growth rate of the (0001) and $\{10\bar{1}1\}$ planes amplifies facet formation and can create a pinhole [15]. A different model has been developed for the V-shaped InGaN defects [17]: in that case, it has been calculated that the energy of the In-covered $\{10\bar{1}1\}$ InGaN planes is lower than that of the In-covered (0001) plane, i.e. that facet formation is energetically favorable. To date, no calculation of the full energy hierarchy of the GaN planes is available, except for the result that the surface energy of the $\{10\bar{1}1\}$ facets is higher than that of the (0001) plane [17].

While the surface morphologies of GaN grown in regimes A and B at $T_S = 730$ °C are similar (Fig. 5), the growth kinetics are rather different. This is demonstrated in Fig. 6, which shows the specular RHEED intensity during GaN growth in the different regimes. Under N-rich conditions (regime A), persistent oscillations are observed, characteristic of a layer-by-layer growth mode by

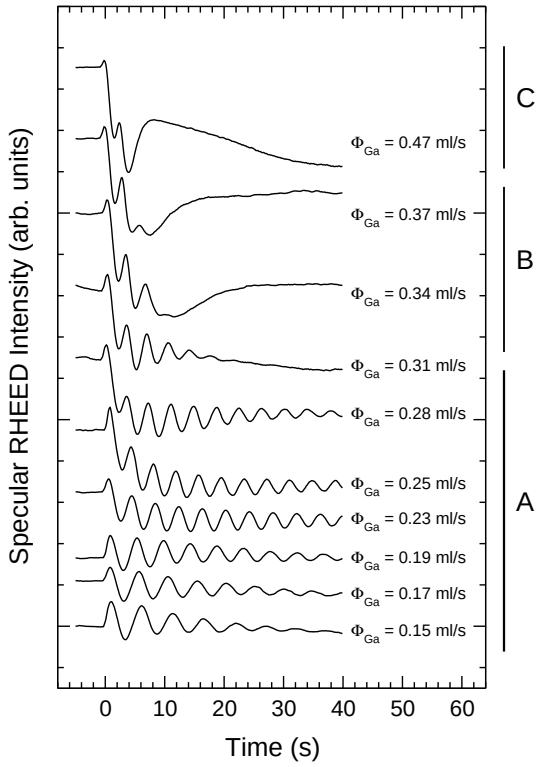

FIG. 6: Specular RHEED intensity obtained during GaN growth at different Ga fluxes, as indicated. $T_S = 730$ °C. The Ga flux ranges for regimes A,B, and C are indicated (see Fig. 3).

monolayer island nucleation and coalescence. In contrast, as soon as the growth conditions become Ga-rich (regimes B and C), RHEED oscillations are rapidly damped or are not observed at all. This can be explained by a growth mode change to a step-flow mode, maybe due to an increase in adatom mobility on Ga-rich surfaces [4, 5]. Despite the apparent change in growth kinetics, the final surfaces after 1 μm of GaN growth in regions A and B are very similar, which suggests that too low an adatom mobility may not be the driving force for pinhole formation and surface roughening at high substrate temperature.

It is worth noting that the surface morphology of GaN layers grown in the N-rich regime A strongly depends on the substrate temperature. This is evidenced in Fig. 7, which shows the AFM image of a 200 nm thick GaN layer grown under N-rich conditions at $T_S = 630$ °C, i.e. at much lower temperature than the sample shown in Fig. 5(a). In contrast to higher substrate temperatures, Bragg spots appear in the RHEED pattern in the incipiency of GaN growth after a few monolayers. The final surface morphology is not characterized by pinholes but by small islands, about 50 nm wide and 5–7 nm high.

Such a surface morphology is close to what one would expect from the theoretical considerations of Zywietz *et al.* [4] who found a low Ga and N adatom mobility on N-rich (0001) GaN surfaces. Low adatom mobility would lead to a high island nucleation rate and to multilayer growth, i.e. GaN islanding, in keeping with the rapid roughening of the growing GaN surface observed by RHEED.

This suggests that indeed adatom mobility may be very low at temperatures around $T_S = 630$ °C, perhaps of the order of the observed island size, i.e. a few 10 nm. However, as stated above, at higher temperatures ($T_S = 730$ °C), the thermally activated diffusion seems rapid enough to produce smooth $\{10\bar{1}3\}$ facets on a length scale of the order of some 100 nm, particularly in regime B.

We will now discuss the surface morphologies obtained in more Ga-rich conditions. Fig. 8 shows the morphology of the surface of the sample grown under Ga-rich conditions with a Ga bilayer present (regime C). The surface is much smoother than that obtained in regimes A and B and is characterized by about 1000 Å wide terrasses, separated by 5 Å high bimolecular steps. Additionally, spiral growth around screw disclocations is occasionally observed.

A special feature are hexagonal nanotube defects, with diameters of about 100 nm at a density of the order of $10^7\,\mathrm{cm}^{-2}$. This nanotubes might be similar to the microtube defects found in 6H-SiC [18]. Previously, GaN nanotubes have also been observed on MOCVD grown GaN samples, however, with diameters much lower than those in the present study [19].

The surface morphology, characterized by atomically-flat terrasses, corroborates the above discussion about the growth mode of GaN. Combined with the non-observation of RHEED oscillations, this supposes that GaN grows in a step-flow mode under such conditions (high T_S, Ga-rich).

The morphology of the surface obtained in the Ga-droplet regime D (see Fig. 9) is characterized by similar terrasses and spiral hillocks. In contrast to the sample

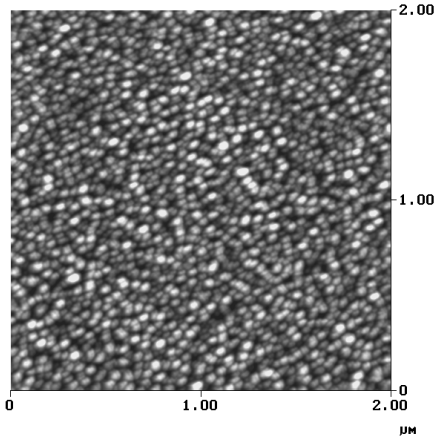

FIG. 7: Atomic-force micrograph of a GaN surface grown under N-rich conditions at a lower substrate temperature of $T_S = 630$ °C. The z-scale is 15 nm.

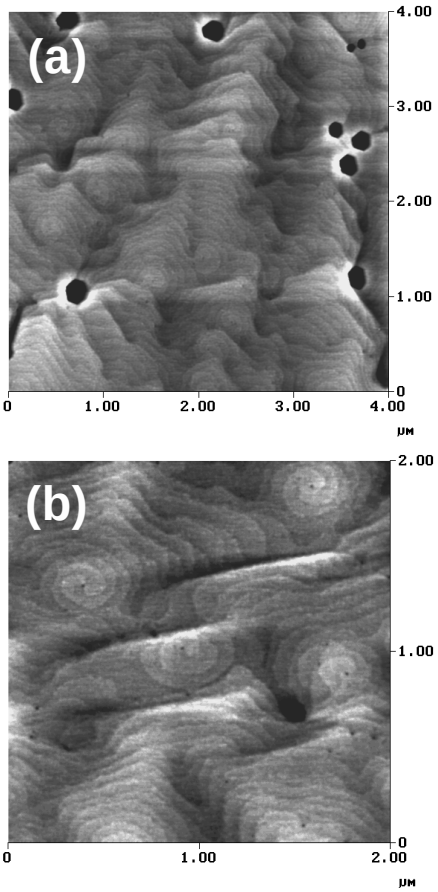

FIG. 8: Atomic-force micrographs of the surface of a sample grown under Ga-rich conditions (Ga bilayer coverage, growth phase diagram region C). The morphology is characterized by about 1000 Å wide terrasses. The z-scales are 8 nm and 5 nm, respectively.

grown in region C, no hexagonal nanotubes are observed on larger images. Some small islands are visible on the terrasses, which may be interpreted as small excess Ga clusters that act as precursors for Ga droplets.

The typical size of the "macroscopic" Ga droplets observed on the sample grown in regime D is of the order of 3–5 μm at a density of the order of $10^5\,\mathrm{cm}^{-2}$, as determined by optical microscopy.

VI. CONCLUSION

In conclusion, we have discussed the Ga surface coverages during GaN homoepitaxy by PAMBE using different Ga/N flux ratios. We have shown that, under moderately Ga-rich conditions, dynamically stable Ga surface coverages can be obtained. Under strongly Ga-rich conditions, infinite Ga accumulation and droplet formation occurs.

The Ga coverages during GaN growth were divided into four regions for sufficiently high substrate temperature:

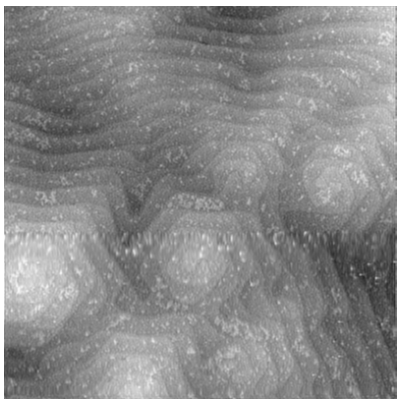

FIG. 9: $1 \times 1\,\mu$m scanning-tunneling micrograph of a sample grown in Ga-droplet conditions (region D).

A. N-rich growth with presumably negligible Ga surface coverage

B. Ga-rich growth with a Ga surface coverage of less than a bilayer

C. Ga-rich growth with the GaN surface covered by a Ga bilayer

D. Ga-rich growth without a stable finite Ga surface coverage and accumulation of Ga into droplets.

The transition lines between the different growth regimes were measured as a function of the substrate temperature, giving rise to a GaN growth phase diagram. For temperatures below 680 °C, regimes B and C are obtained in a tiny range of the Ga/N flux ratio, so only regions A and D are observed in practice.

We have investigated the growth kinetics in the different growth regimes. In regime A, persistent RHEED oscillations are observed, characteristic of a layer-by-layer growth. In the other three regimes, no oscillations are observed, which can be interpreted by the occurence of a step-flow growth mode. We have also investigated the maximum growth rate at the transition between regimes A and B, i.e. at the Ga/N stoichiometry, and we have demonstrated a decrease of the growth rate, which can be interpreted by GaN reevaporation.

Furthermore, we discuss the different GaN surface morphologies obtained after GaN homoepitaxy in the different regions of Ga surface coverage. Growth in region A leads to the formation of inverted pyramids with $\{10\bar{1}3\}$ facets at high substrate temperatures ($T_S = 730$ °C) and flat islands at low substrate temperatures ($T_S = 630$ °C). Region B is characterized at $T_S = 730$ °C by the same inverted pyramids observed in region A.

Whereas growth in regions A and B leads to rough GaN surfaces, growth in regions C and D leads to flat surfaces, characterized by about 1000 Å wide terrasses.

Region C is a good candidate for the long sought GaN growth window' since, in this region, the Ga surface coverage is independent of small fluctuations in Ga flux (see Fig. 2) and substrate temperature (see Fig. 3). Apart from the nanotube defects, the surface morphology is flat and no Ga droplets are observed. If these nanotube defects can be avoided, growth in region C will be a simple method to obtain reproducibly optimum homoepitaxial GaN growth.

ACKNOWLEDGMENTS

We acknowledge O. Briot (University of Montpellier) for supplying the GaN templates and N. Magnea (CEA Grenoble, SP2M) for the use of the STM facility. We would also like to thank J. Neugebauer (Fritz-Haber Institut, Berlin) and F. Rieutord (CEA Grenoble, DRFMC/SI3M) for valuable discussions.

REFERENCES

[1] E. J. Tarsa, B. Heying, X. H. Wu, P. Fini, S. P. DenBaars, and J. S. Speck, J. Appl. Phys. **82**, 5472 (1997).

[2] B. Heying, R. Averbeck, L. F. Chen, E. Haus, H. Riechert, and J. S. Speck, J. Appl. Phys. **88**, 1855 (2000).

[3] B. Heying, I. Smorchkova, C. Poblenz, C. Elsass, P. Fini, S. DenBaars, U. Mishra, and J. S. Speck, Appl. Phys. Lett. **77**, 2885 (2000).

[4] T. Zywietz, J. Neugebauer, and M. Scheffler, Appl. Phys. Lett. **73**, 487 (1998).

[5] T. Zywietz, J. Neugebauer, M. Scheffler, J. E. Northrup, Huajie Chen, and R. M. Feenstra (unpublished).

[6] C. Kruse, S. Einfeldt, T. Böttcher, D. Hommel, D. Rudloff, and J. Christen, Appl. Phys. Lett. **78**, 3827 (2001).

[7] A. R. Smith, R. M. Feenstra, D. W. Greve, M. S. Shin, M. Skowronski, J. Neugebauer, and J. E. Northrup, J. Vac. Sci. Technol. B **16**, 2242 (1998).

[8] G. Mula, C. Adelmann, S. Moehl, J. Oullier, and B. Daudin (unpublished).

[9] J. E. Northrup, J. Neugebauer, R. M. Feenstra, and A. R. Smith, Phys. Rev. B **61**, 9932 (2000).

[10] C. Adelmann, R. Langer, G. Feuillet, and B. Daudin, Appl. Phys. Lett. **75**, 3518 (1999).

[11] M. Zinke-Allmang, L. C. Feldman, and M. H. Grabow, Surf. Sci. Rep. **16**, 377 (1992).

[12] S. Guha, N. A. Bojarczuk, and D. W. Kisker, Appl. Phys. Lett. **69**, 2879 (1996).

[13] N. Grandjean, J. Massies, F. Semond, S. Yu. Karpov, and R. A. Talalaev, Appl. Phys. Lett. **74**, 1854 (1999).

[14] O. Briot, in: *Group III Nitride Semiconductor Compounds*, edited by B. Gil (Oxford Univ. Press, Oxford, 1998), p. 73.

[15] Z. Liliental-Weber, Y. Chen, S. Ruvimov, and J. Washburn, Phys. Rev. Lett. **79**, 2835 (1997).

[16] Y. Chen, T. Takeuchi, H. Amano, I. Akasaki, N. Yamada, Y. Kaneko, and S. Y. Wang, Appl. Phys. Lett. **72**, 710 (1998); X. H. Wu, C. R. Elsass, A. Abare, M. Mack, S. Keller, P. M. Petroff, S. P. DenBaars, J. S. Speck, and S. J. Rosner, *ibid.* **72**, 692 (1998).

[17] J. E. Northrup and J. Neugebauer, Phys. Rev. B **60**, R8473 (1999).

[18] V. G. Bhide, Physica **24**, 817 (1958).

[19] W. Qian, K. Skowronski, M. de Graef, K. Doverspike, L. B. Rowland, and D. K. Gaskill, Appl. Phys. Lett. **66**, 1252 (1995).